Langmuir

ARTICLE

pubs.acs.org/Langmuir

# Silane Layers on Silicon Surfaces: Mechanism of Interaction, Stability, and Influence on Protein Adsorption

Nesrine Aissaoui,[†,‡,§] Latifa Bergaoui,[§] Jessem Landoulsi,[†,‡] Jean-François Lambert,[†,‡] and Souhir Boujday*[,†,‡]

[†]Laboratoire de Réactivité de Surface, UMR 7197, Université Pierre et Marie Curie (UPMC), Université Paris VI, F75005 Paris, France

[‡]Laboratoire de Réactivité de Surface, CNRS, UMR 7191, F75005 Paris, France

[§]Département de Génie Biologique et Chimique, Institut National des Sciences Appliquées et de Technologie (INSAT), Centre Urbain Nord, BP 676, 1080 Tunis Cedex, Tunisia

**ABSTRACT:** In this work the mechanism of (3-aminopropyl)triethoxysilane (APTES) interaction with silicon surfaces is investigated at the molecular level. We studied the influence of experimental parameters such as time, temperature, and concentration on the quality of the APTES layer in terms of chemical properties, morphology, and stability in aqueous medium. This was achieved using a highly sensitive IR mode recently developed, grazing angle attenuated total reflection (GA-ATR). This technique provides structural information on the formed APTES layer. The topography of this layer was investigated by atomic force microscopy in aqueous medium. The hydrophilicity was also studied using contact angle measurement. Combining these techniques enables discussion of the mechanism of silane grafting. Considerable differences were observed depending on the reaction temperature, room temperature or 90 °C. The data suggest the presence of two adsorption sites with different affinities on the oxidized silicon layer. This also allows the optimal parameters to be established to obtain an ordered and stable silane layer. The adsorption of proteins on the APTES layer was achieved and monitored using in situ quartz crystal microbalance with dissipation monitoring and ex situ GA-ATR analyses.

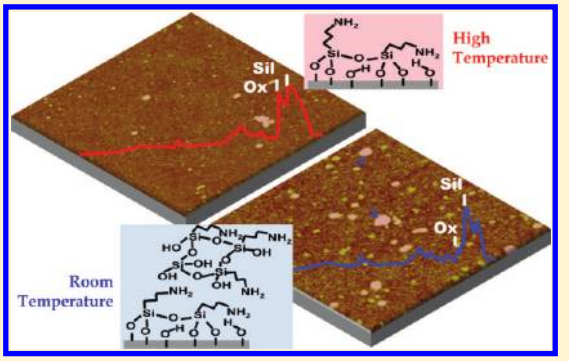


## 1. INTRODUCTION

The immobilization of biomolecules on solid surfaces has been the subject of extensive research owing to its importance in materials science and biological applications.[1] Generally, surfaces are chemically modified to better control the organization and the orientation of immobilized species, thus optimizing their biologic functions. This can be easily achieved on gold by constructing more or less ordered self-assembled monolayers (SAMs) of thiols,[2−4] and several studies correlated the efficiency of biomolecules to the composition, thickness, and order of the SAM.[5−9] On silicon surfaces, the most common route of functionalization is to attach alkylsilanes through the formation of Si−O−Si bonds between the silanol groups present on the oxidized silicon surface and the hydrolyzed organosilane molecules.[10−12]

This reaction is complex, and the silane retention and organization on the surface are still under debate.[11−15] Indeed, various interfacial processes may be possible (covalent binding to the surface, lateral polymerization of adsorbed silanes, three-dimensional polymerization, etc.) depending on the nature of the reactive moieties bound to Si in the silane (typically Cl or an alkoxy group), on their number, and more generally on the experimental parameters.

(3-Aminopropyl)triethoxysilane (APTES) is one of the most widely used organosilane agents for the preparation of amine-terminated films. The presence of $-NH_2$ end groups on the surface has a major importance in biological applications as it allows protein or other biomolecules to be attached in a simple way. Many studies have been reported in the literature showing the relevance of APTES use for the immobilization of different entities with biologic interest on various substrates (refs 16−23 and references therein). The structure of APTES-derived films is complex. Schematically, silane grafting is expected to occur in two steps in the presence of water molecules.[16] First, the ethoxy groups are hydrolyzed, either in the liquid phase or at the interface, depending on the experimental procedure. Second, Si−O−Si bonds are formed with surface silanol groups. However, these processes are difficult to evidence and strongly depend on the hydration state. One major problem is associated with the ability of the precursor to copolymerize in the presence of traces of water, thus forming aggregates and disordered layers on the substrate; conversely, in conditions of very low water activity, grafting could occur through direct nucleophilic attack of the surface groups (silanols) on the silane molecules without intermediary hydrolysis. Furthermore, the silane layer may be unstable in the aqueous media used for biological applications: partial hydrolysis

**Received:** September 20, 2011
**Revised:** November 21, 2011
**Published:** November 22, 2011

of the siloxane bonds may cause desorption.[24,25] One of the most widely used techniques to investigate silane grafting on planar silicon surfaces is Fourier transform IR spectroscopy, which provides crucial structural information on the silane layer. However, the conventional modes, namely, transmission and/or attenuated total reflection (ATR), lack sensitivity. Recently, a considerable enhancement of sensitivity was achieved using a high refractive index germanium crystal. A new IR mode, grazing angle attenuated total reflection (GA-ATR), leading to an enhancement in sensitivity to a factor 100 when compared to conventional IR modes, was described by Lummerstorfer et al. and Milosevicet et al.[26−29]

Our aim in the present work is to investigate at the molecular level the mechanism of silane interaction with a silicon surface. The influence of experimental parameters (time, temperature, concentration) on the quality of the APTES layer in terms of morphology, chemical properties, and stability in aqueous medium is explored. To this end, IR in GA-ATR mode is used to obtain the structural information. The topography of the obtained APTES film is examined by atomic force microscopy (AFM) in the aqueous medium. The hydrophilicity of the APTES layer is studied using contact angle measurement. Combining these techniques enables better understanding of the mechanism of silane grafting and thus establishment of the optimal parameters to obtain an ordered and stable silane layer. Eventually, these platforms are used for the adsorption of proteins, and the latter process is monitored using in situ quartz crystal microbalance with dissipation monitoring (QCM-D) and ex situ GA-ATR analyses.

## 2. MATERIALS AND METHODS

**2.1. Materials.** Silicon wafers ⟨100⟩ from Sigma-Aldrich (France) were cut into 1 × 2 $cm^2$ pieces. $Na_2HPO_4$, $NaH_2PO_4$, APTES (98%), and proteins (Candida Antarctica Lipase B, or "CALB", EC 3.1.1.3, 10.8 $U \cdot mg^{-1}$) were purchased from Sigma-Aldrich, $H_2O_2$ (30%) and toluene were purchased from Prolabo (VWR, France), and $H_2SO_4$ (96%) was purchased from Carlo Erba (France).

**2.2. Sample Preparation.** *2.2.1. Silicon Wafer Cleaning.* First, wafer surfaces were cleaned using a sonication bath (70 W, 40 kHz, Branson, Danbury, CT) in acetone for 10 min and then in a binary mixture of acetone and ethanol (50/50) for 10 min and rinsed abundantly with ultrapure water (Milli-Q, Millipore, France). Second, samples were immersed in freshly prepared piranha solution (30% $H_2O_2$ and 96% $H_2SO_4$, 1:3) for 15 min. (*Caution: piranha solution is a strong oxidant and reacts violently with organic substances!*) These substrates were then thoroughly washed in ultrapure water and dried under nitrogen gas flow. Finally, the samples were treated for 2 h in a UV-ozone cleaner (Bioforce Nanoscience) and then stored in ultrapure water.

*2.2.2. Silane Grafting Procedures.* APTES grafting on silicon wafers was achieved by exploring three main parameters (APTES concentration, silanization time, and silanization temperature) as follows:

| Silane concentration | | Reaction time | | Reaction temperature |
|---|---|---|---|---|
| 1, 10, and **50 mM** | → | 1, 3, 6, **12** and 24 h | → | RT, 90°C |

All the solutions were prepared in toluene. Silane grafting (silanization) was performed, first at room temperature, by immersing the cleaned silicon wafer in the APTES solution with immersion times varying from 1 to 24 h. In a later step (see the Results), the optimum conditions of concentration and time (50 mM, 12 h) were tested both at room temperature (RT) and at 90 °C (HT). After the silanization step, the samples were sonicated for 10 min in anhydrous toluene, dried under nitrogen, and heated in an oven at 90 °C for 2 h, unless stated otherwise.

*2.2.3. Protein Adsorption.* Protein adsorption was achieved by depositing 200 μL of the CALB solutions (100 $\mu g \cdot mL^{-1}$, in phosphate buffer) on the functionalized silicon surfaces at room temperature for different times (from 5 min to 24 h). Samples were then thoroughly rinsed with Milli-Q water.

**2.3. GA-ATR Analyses.** IR spectra were obtained by working with a GA-ATR accessory. The experimental setup is described in detail in refs 26, 28, and 29. All the spectra were recorded using the VariGATR (Harrick Scientific, Pleasantville, NY) equipped with a horizontal reflection ATR accessory including a germanium crystal. The spectrometer is equipped with a nitrogen-cooled mercury−cadmium−telluride (MCT) wide-band detector. The silicon wafer sample is placed face-down on the Ge crystal, and a force is applied via the pressure tip. The angle of incidence is fixed at 65°. IR spectra were recorded in a wavelength range from 600 to 4000 $cm^{-1}$. For each spectrum, 256 scans were collected with a nominal resolution of 8 $cm^{-1}$. The background was recorded on the GA-ATR unit without any substrate pressed against the crystal.

**2.4. QCM-D.** The adsorption of protein on silicon substrate was followed in situ by quartz crystal microbalance with dissipation monitoring. Measurements were performed with a Q-Sense E1 system (Gothenborg, Sweden) at a temperature of 24.0 ± 0.1 °C. The crystal used was a thin AT-cut quartz coated with a thin $SiO_2$ film (thickness ∼50 nm) provided by Q-Sense. It was cleaned as previously described for silicon wafers. Oscillations of the crystal at the resonant frequency (5 MHz) or at one of its overtones (15, 25, 35, 45, 55, and 65 MHz) were obtained when applying ac voltage. The variations of the resonant frequency ($\Delta F$) and of dissipation ($\Delta D$) were monitored upon adsorption of the proteins. Solutions were injected into the measurement cell using a peristaltic pump (Ismatec IPC-N 4) at a flow rate of 50 μL/min. Prior to the protein adsorption, a phosphate buffer solution was injected to avoid any perturbation in frequency due to the medium change. The protein solution was then brought into the measurement cell until the frequency and dissipation signal reached a stationary value. Subsequently, rinsing was performed using phosphate buffer solution. The presented data correspond to the third overtone.

**2.5. Water Contact Angle Measurements.** Static water contact angles were measured at room temperature using the sessile drop method and image analysis of the drop profile. The instrument, using a charge-coupled device (CCD) camera and an image analysis processor, was purchased from Krüss (Germany). The water (Milli-Q) droplet volume was 1 μL, and the contact angle was measured 5 s after the drop was deposited on the sample. For each sample, the reported value is the average of the results obtained on three droplets and the overall precision in the measurements was better than ±5°.

**2.6. Atomic Force Microscopy.** Atomic force microscopy images were taken using a commercial atomic force microscope (Bruker Nano Inc.-Nano Surfaces Division) equipped with a 150 × 150 × 5 μm scanner (J-scanner). A quartz fluid cell was used without the O-ring. The substrates were fixed on a steel sample puck using a small piece of adhesive tape. The mounted samples were immediately transferred into the AFM liquid cell while avoiding dewetting. Topographic images were recorded in tapping mode in phosphate buffer at room temperature (21−24 °C) using oxide-sharpened microfabricated $Si_3N_4$ cantilevers (Santa Barbara, CA). The spring constants of the cantilevers, measured using the thermal noise method, were found to be close to 0.05 N/m. The curvature radius of the silicon nitride tips was about 20 nm (supplier specifications). All images shown in this paper are flattened data using a third-order polynomial.

## 3. RESULTS

**3.1. IR Vibrational Features and Chemical Functions.** Figure 1A, curve a, shows a typical spectrum for a pretreated


dx.doi.org/10.1021/la2036778 |*Langmuir* 2012, 28, 656–665

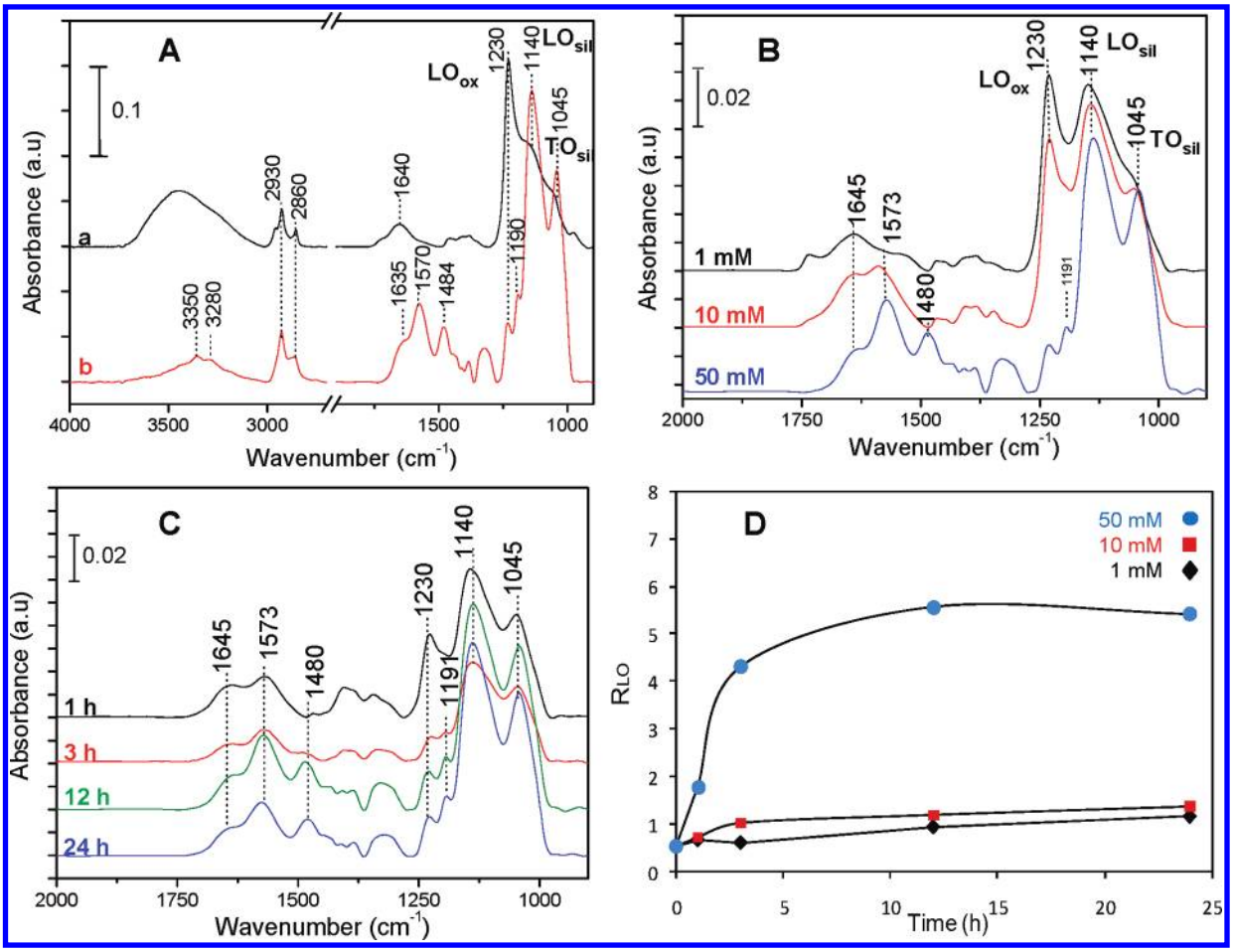


**Figure 1.** GA-ATR spectra: (A) before (a) and after (b) silane grafting at $C$ = 50 mM and $t$ = 12 h at room temperature, (B) room-temperature silanization at various APTES concentrations, (C) room-temperature silanization at various times, (D) evolution of the ratio $R_{LO}$ as a time function from panels B and C. LO$_{ox}$, LO$_{sil}$, and TO$_{sil}$ refer to LO and TO modes in the native oxide and silane layers, respectively.

silicon wafer. Despite the extensive pretreatment, some contaminants are still present on the surface as evidenced by the symmetric and asymmetric $\nu(CH_2)$ observed at 2930 and 2860 cm$^{-1}$, respectively. The hydroxyl group and hydrogen-bonded water molecule give bands in the 3600 cm$^{-1}$ region. These water molecules also give additional bands at 1640 cm$^{-1}$.[30,31] The most relevant wavenumber range is from 950 to 1250 cm$^{-1}$ as it includes Si−O−Si vibrational modes.[18,20,32−34] The oxidized silicon surface is dominated in this range by a strong band at 1230 cm$^{-1}$ with a smaller one at 1045 cm$^{-1}$. These features are usually interpreted assuming a continuous silica layer.[18,20,23,35−37] The vibrational properties of bulk silica are rather well-known:[38,39] in silica, the asymmetrical Si−O−Si stretch undergoes a phonon splitting between longitudinal optic (LO) and transverse optic (TO) components. It has been shown[40,41] that, in a thin $SiO_2$ film, the TO vibrations are parallel to the film surface while the LO vibrations are perpendicular to it. The band at 1230 cm$^{-1}$ is assigned to the LO mode of the unfunctionalized silica surface and the band at 1045 cm$^{-1}$ to the corresponding TO mode. A residual absorption around 1100 cm$^{-1}$ may be due, e.g., to $\nu'_a$ vibrations of "anchored" Si−O−Si units as proposed in ref 39.

After silane grafting at room temperature (Figure 1A, curve b), the intensity of the 1230 cm$^{-1}$ band is strongly attenuated while a strong band appears at ∼1140 cm$^{-1}$. In the literature this band has been assigned to the LO stretching modes in the growing layer created by APTES condensation reactions,[18,33,35,42] while the TO mode of the same layer, at 1045 cm$^{-1}$, is not distinguishable from the corresponding mode of the unsilanized surface. This assignment rests on the supposition that the growing silanized layer has sufficient lateral connectivity for long-range interactions to take place. This spectral region also exhibits a small band at ∼1190 cm$^{-1}$ due to the $CH_2$ rocking mode of unreacted ethoxy groups ($SiO-CH_2-CH_3$).[18,33,35,42−44] The $NH_2$ scissor vibration found at 1570 cm$^{-1}$ confirms the presence of the terminal groups of the APTES molecules after grafting. In addition to this mode, other features at 1484 and 1635 cm$^{-1}$ correspond to the symmetric and asymmetric $-NH_3^+$ deformation modes, indicative of amine group protonation when the samples are exposed to air.[18,34]

Around 3280 and 3350 cm$^{-1}$, the symmetric and asymmetric NH stretch modes of the amino groups are very weak in intensity because of their weak dipole moment.[20] $CH_2$ asymmetric and symmetric stretching modes are observed at 2930 and 2860 cm$^{-1}$, respectively. They could be due to the presence of the propyl chains of the APTES molecules even though the organic contamination, already observed on pretreated silicon, cannot be excluded.

It is worth noting that, under grazing angle incidence, the p-polarized light is highly sensitive to surface IR absorption, leading to a significant enhancement of components perpendicular to


dx.doi.org/10.1021/la2036778 |Langmuir 2012, 28, 656–665

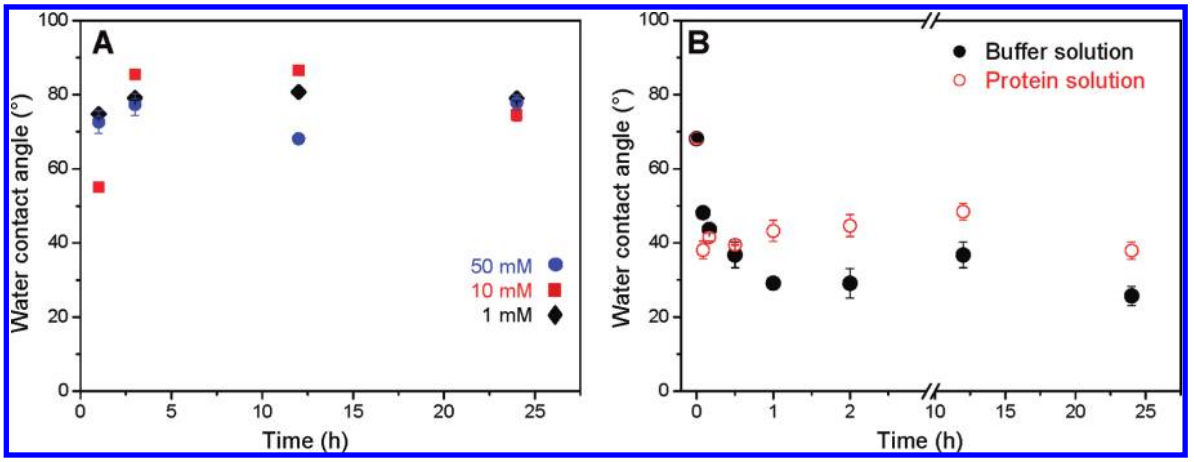


**Figure 2.** Water contact angle measurements: (A) at different concentrations of APTES as a function of the reaction time, (B) as a function of the conditioning time in protein solution or in phosphate buffer.

the surface plane.[28,29,45,46] This makes the exploitation of the perpendicularly oriented LO mode bands particularly relevant, since they are intense and allow the discrimination between signals originating from the underlying silicon oxide (at 1230 $cm^{-1}$) and from the silane layer (at 1140 $cm^{-1}$), whereas in contrast the TO modes are hardly distinct in both cases. Therefore, to investigate the silane layer evolution in a semiquantitative way, we defined the band intensity ratio, $R_{LO}$, as follows:

$$R_{LO} = \frac{I_{1140}}{I_{1230}}$$

where $I_{1140}$ and $I_{1230}$ are the intensities relative to LO bands of Si−O−Si groups in the silane layer and the silicon oxide, respectively. This $R_{LO}$ ratio is a rough indicator, but it makes the meaning of the results appear more concretely and provides relevant information regarding the silane layer growth. It should be noted that $R_{LO}$ is not linearly proportional to the silane layer thickness; as the latter increases, $I_{1140}$ will increase but at the same time $I_{1230}$ will decrease.

**3.2. Influence of Experimental Parameters on Silane Grafting.** Three experimental parameters were explored for silane grafting: concentration, time, and temperature. GA-ATR IR spectra obtained after 12 h of reaction at room temperature for different APTES concentrations (1, 10, and 50 mM) are shown in Figure 1B. All the spectra show the same vibrational features. The LO and TO vibrational modes at 1140 and 1045 $cm^{-1}$ increase in intensity with the APTES concentration. We fixed the silane concentration at 50 mM and systematically increased the reaction time (1, 3, 12, and 24 h): the corresponding spectra are shown in Figure 1C. Here again, the LO and TO vibrations increase with reaction time and seem to stabilize at 12 h, suggesting a successful grafting of silane in these conditions, i.e., 50 mM and 12 h.

The evolution of $R_{LO}$ for these spectra is shown in Figure 1D. In this figure one can observe an appreciable increase of $R_{LO}$ as a function of the reaction time to reach a plateau after 12 h. This tendency is the same for all silane concentrations, but the final value of $R_{LO}$ at the plateau is noticeably higher for a silane concentration of 50 mM.

Water contact angle measurements for these different experimental conditions are shown in Figure 2A. The pretreated silicon surface was very hydrophilic, and a contact angle could not be measured due to drop spreading.

Figure 2A shows that contact angles increase with reaction time, suggesting that surfaces progressively become less hydrophilic due to the presence of more or less ordered APTES chains. While this tendency is in agreement with IR data, the effect of the silane concentration is much less dramatic for contact angles than for IR. The samples obtained for all three concentrations seem to converge to the same degree of hydrophilicity, probably corresponding to a full lateral coverage of the surface by silane groups. The higher value of $R_{LO}$ for high concentrations would then be attributed to the formation of silane layers with higher (average) thickness. Following this interpretation, it can also be seen from Figure 2A that full surface coverage is reached faster for the highest concentration (compare the values after 1 h of reaction).

In all the following experiments, silane grafting was carried out for 12 h starting from a 50 mM APTES solution.

**3.3. Silane Layer Stability in Buffer Solution.** In a first attempt at protein adsorption on the silane layers, a series of silicon surfaces functionalized at RT were incubated from 10 min to 12 h in a protein solution in phosphate buffer and then rinsed and dried as described in the Materials and Methods. The resulting GA-ATR IR spectra are shown in Figure 3A. At the same time, to assess the stability of the APTES layer in the buffer, the same incubation conditions were applied to another series in buffer but without addition of proteins (Figure 3B).

For both cases, IR spectra show a similar evolution: starting from the first 10 min of incubation time, the shoulder at 1190 $cm^{-1}$ that we assigned to surface-grafted but incompletely hydrolyzed APTES disappeared probably due to its complete hydrolysis. At the same time, a progressive decrease of the intensity of the vibrational modes assigned to the deformation modes of $NH_2$ at 1570 $cm^{-1}$ and $NH_3^+$ at 1645 and 1480 $cm^{-1}$ is observed, suggesting the progressive removal of grafted silane molecules from the surface. For both cases we also observe a modification of the relative intensities of these bands: the $NH_2$ band at 1570 $cm^{-1}$ became the less intense one, suggesting that the remaining amine groups are all protonated. In addition, only the asymmetric vibrations of $NH_3^+$ at 1645 $cm^{-1}$ are still visible: these groups could be involved in ionic interaction with $HCO_3^-$ derived from ambient $CO_2$ as previously hypothesized by Culler et al.[47]

When samples are incubated in the protein solution, (Figure 3A), the interpretation is not straightforward because of possible band overlap. The IR features of amide bands associated with the


dx.doi.org/10.1021/la2036778 |*Langmuir* 2012, 28, 656–665

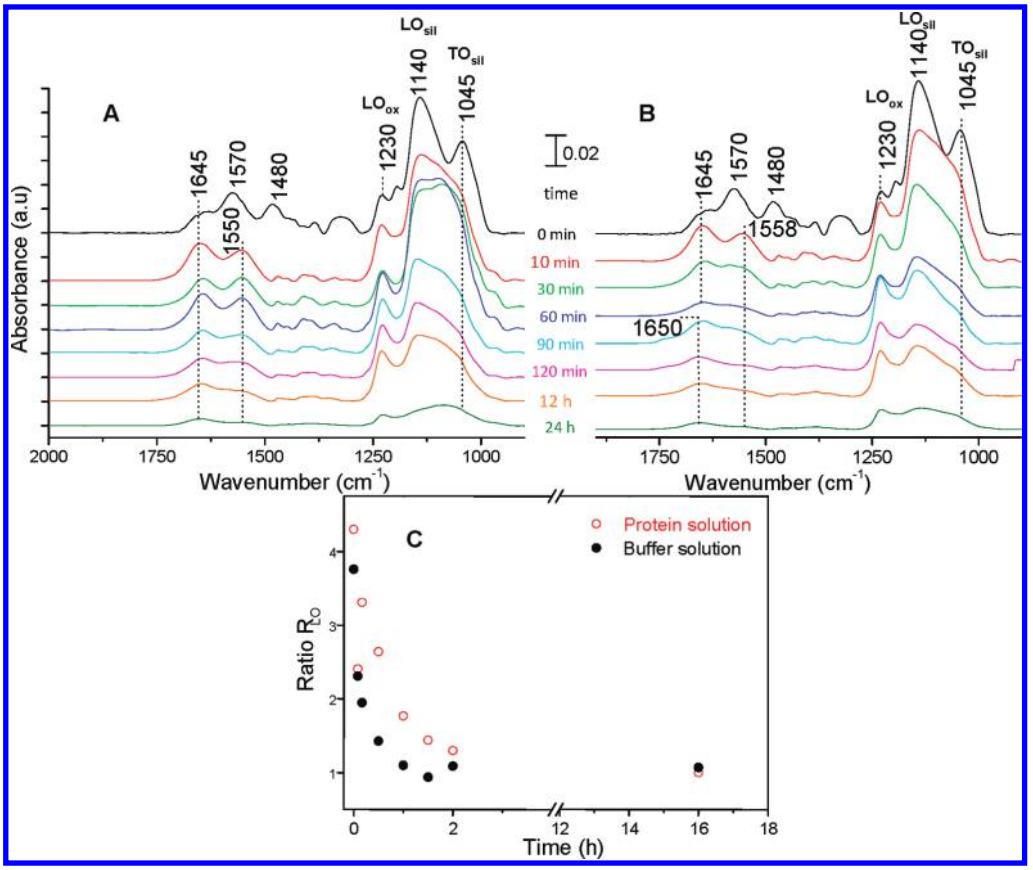


**Figure 3.** GA-ATR spectra recorded on room-temperature silanized samples prior to and after conditioning for various incubation times in protein solution (A) or in buffer (B). (C) evolution of $R_{LO}$ from panels A and B. $LO_{ox}$, $LO_{sil}$, and $TO_{sil}$ refer to LO and TO modes in the native oxide and silane layers, respectively.

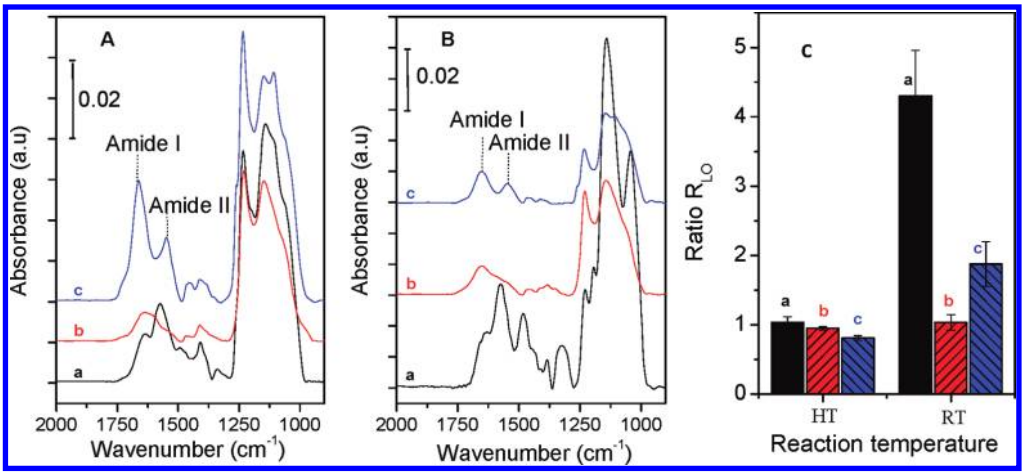


**Figure 4.** (A) GA-ATR IR spectra after silanization at high temperature (a) and incubation in buffer (2 h) (b) and in protein solution (2 h) (c). (B) GA-ATR IR spectra after silanization at room temperature (a) and incubation in buffer (2 h) (b) and buffer (2 h) prior to the incubation in protein solution (2 h) (c). (C) Evolution of $R_{LO}$ from panels A (HT) and B (RT).

presence of proteins are expected at ~1550 cm$^{-1}$ (amide II) and ~1660 cm$^{-1}$ (amide I). Two bands are observed at 1570 and 1645 cm$^{-1}$ in our samples. However, if these features were associated with protein adsorption, they would be expected to either remain constant (in the case of fast adsorption) or increase with contact time, while in fact they decrease at the same rate both in the protein solution and in the reference buffer solution. They must therefore be assigned, as in the original silanized samples, to the terminal $-NH_2$ scissor vibration and the asymmetric $-NH_3^+$ deformation, respectively. The observed decrease corroborates the removal of some grafted silane molecules either in the buffer or in the protein solution, without any detectable protein


dx.doi.org/10.1021/la2036778 |*Langmuir* 2012, 28, 656–665

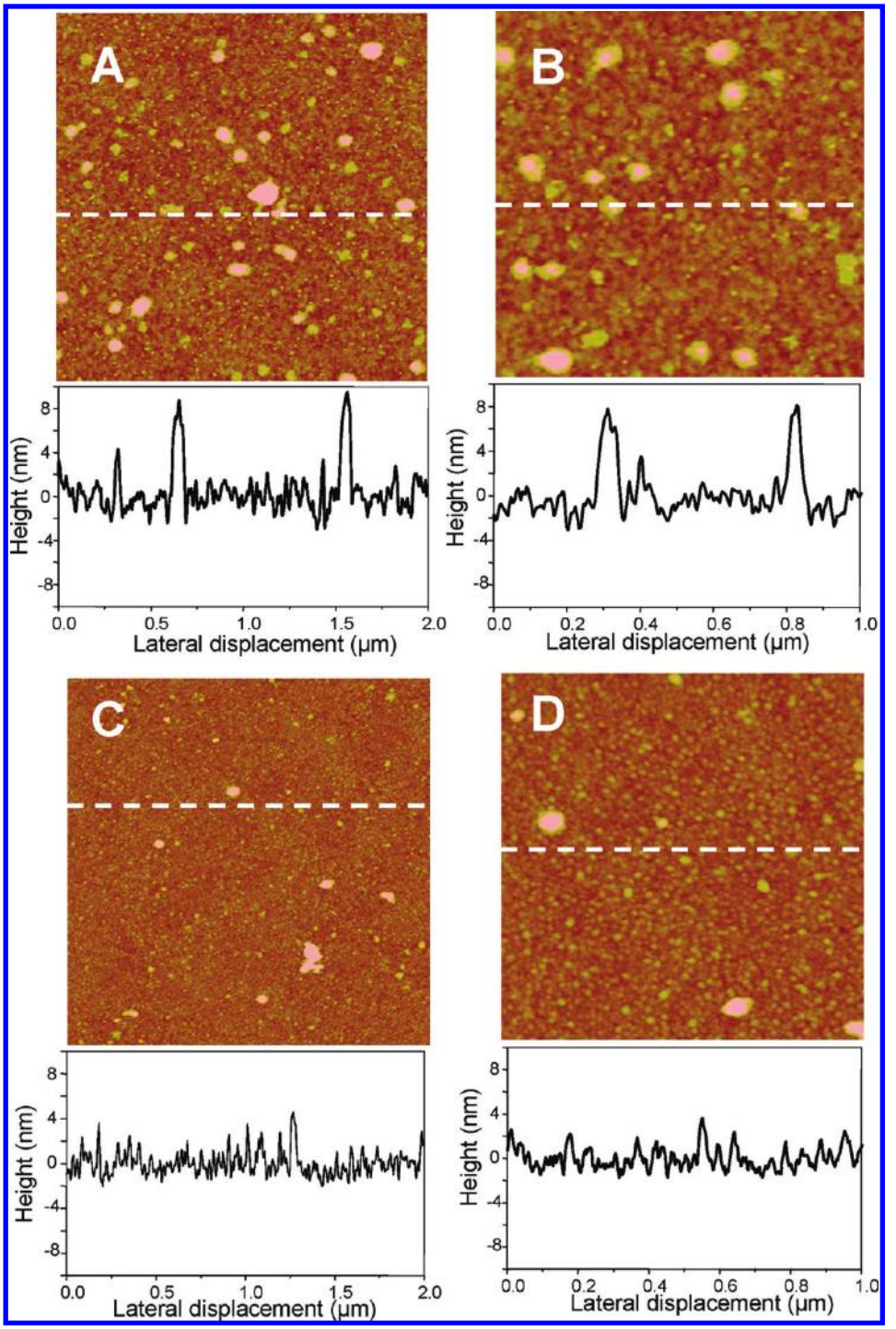


**Figure 5.** AFM height images (tapping mode, in phosphate buffer; *z* scale 20 nm; image size 2 × 2 $\mu m^2$ for panels A and C, 1 × 1 $\mu m^2$ for panels B and D) of (A, B) room-temperature and (C, D) high-temperature silanized silicon wafers. Cross sections were taken at the place indicated by the dashed line.

adsorption. More direct evidence regarding the evolution of the silane layer is given by the evolution of the $R_{LO}$ ratio (Figure 3C). It shows a noticeable decrease of $R_{LO}$ with the incubation time, unambiguously revealing the instability of APTES films in the presence of both the buffer and protein solutions. This evolution is rather fast, being essentially complete after 1 h in the buffer solution; in the protein solution, it is even faster but converges to the same final value.

These results are supported by the evolution of the water contact angle (Figure 2B). After GA-ATR analyses, water contact angles were measured on the same samples. Contact angles decreased from 62 to 25 and 38 for APTES films incubated in the buffer and the protein solution, respectively, indicating that surfaces became much more hydrophilic, which is compatible with the loss of functionalizing molecules.

The question of the stability of the silane layer is of course of primordial importance for the use of functionalized Si platforms. We therefore set out to determine if a different protocol for silane grafting (changing the temperature) had any influence


dx.doi.org/10.1021/la2036778 |*Langmuir* 2012, 28, 656–665

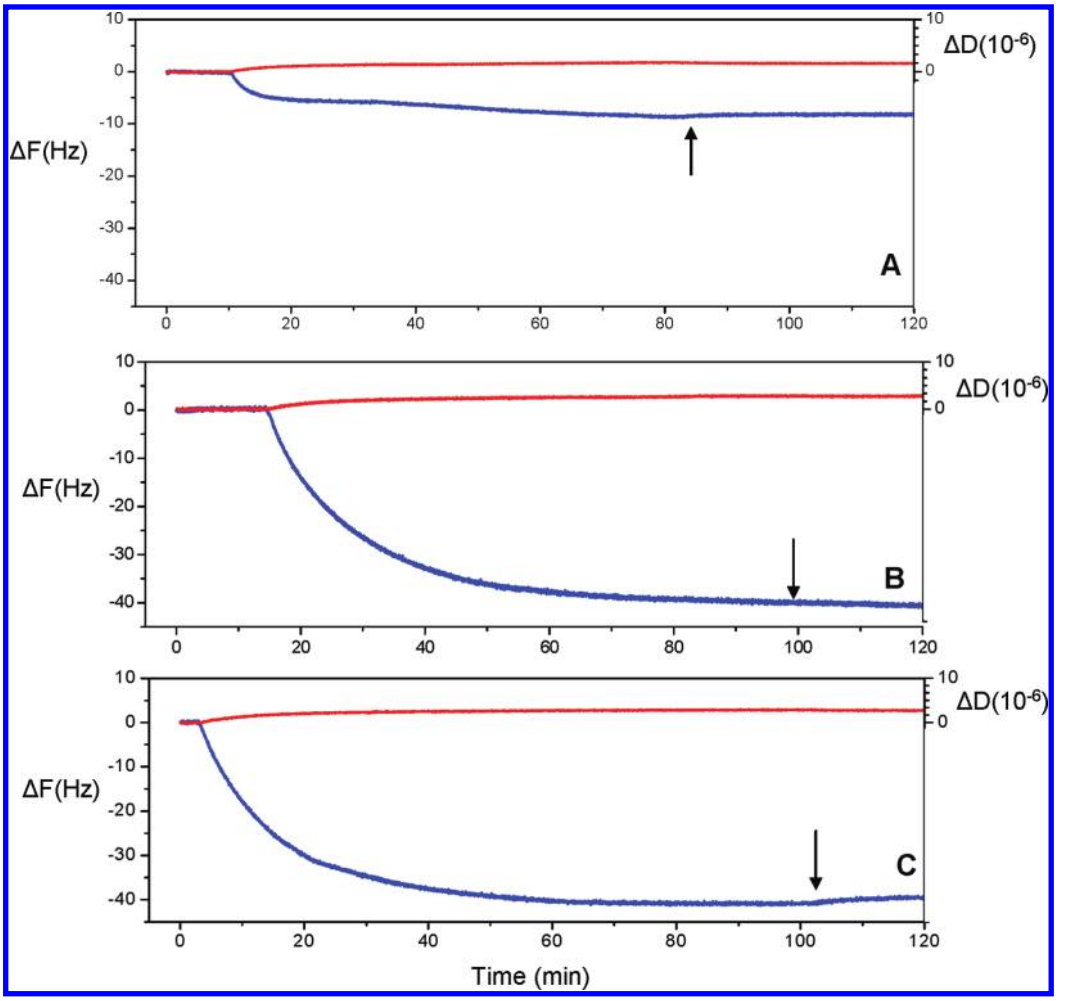


**Figure 6.** QCM-D data obtained during the adsorption of proteins (CALB, buffer pH ≈ 7, 100 $\mu g \cdot mL^{-1}$) on (A) a nonsilanized silicon wafer and (B) room-temperature and (C) high-temperature silanized silicon wafers: lower curves, frequency change; upper curves, dissipation change. Rinsing steps are indicated by arrows.

on the silane layer stability. Interestingly, results given in Figure 4 revealed two relevant features. First, the $R_{LO}$ ratio reached after 12 h of reaction was significantly lower for the HT functionalized sample (Figure 4C). Second, no significant detachment or deterioration of the silane layer was observed while using the HT procedure, independent of the conditioning medium. $R_{LO}$ is kept constant, and the only change in the IR spectra (Figure 4A) concerns the balance between protonated and unprotonated amine groups. Upon incubation in a protein buffer solution, we clearly observe the signature of amide I and II indicating their presence on the surface.

The surface topographies of APTES layers obtained by grafting at room and high temperature were observed using AFM in phosphate buffer solution. Using the RT procedure, we observed the presence of many aggregates with different sizes (Figure 5A). The roughness $R_{rms}$ was 3.14 nm, and cross sections indicated that the aggregates may reach 10 nm in height. The formation of aggregates may result from the physical adsorption on the silicon wafer of silanes prepolymerized in the solution, but it may also be a case of surface nucleation (see below); in fact, the latter explanation appears more likely since this step was carried out in anhydrous conditions, which should not allow silane hydrolysis in the solution.

Upon silane grafting at high temperature, the surface topography was smoother with almost no aggregates (Figure 5C) and the roughness decreased to 1.28 nm. AFM images also showed that working at HT leads to a more homogeneously organized layer (compare panels B and D of Figure 5); the aggregates are less frequent and of smaller size, and their height hardly reaches 4 nm. Furthermore, it must be noted that surface imaging of the RT functionalized samples was made more difficult by the low stability of the silane layer in the buffer, leading to the adsorption of silane compounds on the AFM tip.

**3.4. Adsorption of Proteins.** The adsorption of protein on the APTES-terminated silicon surface using either the RT or the HT procedure was investigated in situ with QCM-D. The adsorption on a nonfunctionalized silicon wafer was also evaluated as a reference. The shifts of the resonant frequency of the third overtone ($\Delta F$) and of the corresponding dissipation change ($\Delta D$) due to the interaction with the protein solution are shown in Figure 6.

On silane-terminated silicon surfaces, $\Delta F$ and $\Delta D$ evolutions were similar to those obtained for other common globular proteins.[48,49] The low change in dissipation is consistent with the adsorption of these small and dense molecules. Final $\Delta F$ values of −40 Hz were obtained and essentially stabilized before the rinsing step. However, on the bare silicon wafer, the frequency shifts were significantly lower and appeared to be more progressive


dx.doi.org/10.1021/la2036778 |*Langmuir* 2012, 28, 656–665

(Figure 6A). Moreover, rinsing seemed to interrupt this evolution at (absolute) $\Delta F$ values lower than 10 Hz.

For the two protocols of silane grafting, the QCM curves are almost identical. This may look surprising when compared to GA-ATR data, but it is important to note at this stage that the stabilization times were very different for the two protocols. Indeed, while the stabilization is almost immediate for the protocol at 90 °C, it was very long for the protocol at RT. The drift in the latter case might result from the removal of some silanes during incubation in the buffer as evidenced previously by IR. However, not all grafted silanes are released, and we can suppose that the remaining silanes are able to successfully bind proteins with the same efficiency as the silane layer built at 90 °C. To validate this hypothesis, we carried out the same experiment (i.e., incubating samples prepared following the RT procedure in the buffer prior to the incubation in the presence of the protein) outside the QCM apparatus and studied the resulting samples by GA-ATR IR. The results, shown in Figure 4B,C, clearly corroborate the QCM data: a decrease in $R_{LO}$ upon incubation followed by the appearance of amide bands, proving the efficient sorption of proteins.

## 4. GENERAL DISCUSSION

We believe that most of our data can be rationalized in a simple nucleation−growth model on a chemically heterogeneous surface. Indeed, it is misleading to view a $SiO_2$ surface as homogeneous, even if the exposed groups are mostly silanols. Different groupings, connectivities, and geometries of these silanol groups give rise to surface sites with significantly different chemical affinities, as was demonstrated in the case of dispersed silica.[50,51] At RT, the kinetics of "condensed silane" nucleation on the surface would be slow, except on a few special sites. After initial, quick nucleation on these special sites, big agglomerates would have significant time to grow on these sites, before nucleation is initiated elsewhere on the surface (on weaker nucleation sites), and such agglomerates are indeed evidenced by AFM. After 10 h, the silane material would then consist of two parts: a more or less homogeneous layer covering the whole surface and protruding 10 nm thick aggregates. The presence of the aggregates contributes to an increase of $R_{LO}$ (ATR data), but they are easily detached upon further treatments, perhaps because there is only one chemical (covalent) anchoring point with the surface and additional interactions that stabilize the aggregates are destroyed upon incubation in the buffer. For silane grafting carried out at 90 °C, on the other hand, nucleation would be fast everywhere on the surface and a laterally homogeneous layer would start growing immediately. Less aggregates would be formed, with lower width and thickness. As a result, the total amount of deposited silanes would be smaller but their structure would be more uniform and more resistant to (water or buffer anion) chemical attack.

The IR data tend to show that the silane overlayer formed at room temperature is very fragile. It is largely eroded on a time scale faster than the hour in solutions at pH 7. This chemical lability has been observed before, and it was proposed that the amine moieties at the end of the flexible chains were able to specifically catalyze the destruction of the siloxane (Si−O−Si) bridges formed during the silane adsorption.[16,52] Alternatively, the amine moieties could be protonated in the buffer, disrupting H-bonds that previously stabilized the large aggregates. It seems however that once the aggregates have been removed the remaining, laterally homogeneous multilayer on the native silica surface is much more resilient and can subside for many hours in the presence of the conditioning solution without much alteration: neither the water contact angles nor $R_{LO}$ is restored to its initial value prior to silane grafting, and in particular the surface hydrophilicity does not increase.

While it has already been observed that loosely bound and strongly bound silane-derived species are formed together on $SiO_2$ surfaces,[35] IR techniques alone would not be able to discriminate between lateral heterogeneity and "transverse" heterogeneity (where the upper layers would be different from the lower ones), because the information they provide is averaged over the whole surface. The combination of GA-ATR with the resolution power of AFM is essential in this respect.

The practical lesson for the preparation of silanized $SiO_2$ platforms is that it is simpler to carry out the silane grafting step at high temperatures, because then a stable silane layer is directly formed. For grafting carried out at room temperature, an additional curing step (e.g., in a buffer solution) would be needed to obtain a stable overlayer prior to further use.

## 5. CONCLUSION

The mechanism of APTES interaction with silicon surfaces was investigated using IR in grazing angle attenuated total reflection mode, atomic force microscopy, and contact angle measurements. The collected data suggest that the mechanism follows a nucleation−growth model on a chemically heterogeneous surface. The nucleation seems to occur on at least two sites with different kinetics. On the high-affinity sites the growth is fast and leads to aggregate formation. These aggregates seem to be stabilized through H-bonds with the terminal amine groups of the surface. Immersion in a buffer solution protonates these amine groups, leading to the removal of the aggregates together with proteins, if present in the buffer. Working at high temperature limits aggregate formation, probably due to the increase of nucleation−growth kinetics on the low-affinity sites, and gives stable silane layers able to bind proteins. Therefore, the practical lesson for the preparation of a stable silane layer on $SiO_2$ platforms is to carry out the silane grafting step at high temperatures. Working at room temperature is also possible but with an additional curing step (e.g., in a buffer solution) prior to further use.

## AUTHOR INFORMATION

### Corresponding Author

*Phone: +33144276001. Fax: +33144276033. E-mail: souhir.boujday@upmc.fr.

## REFERENCES

(1) Kasemo, B. Biological surface science. *Surf. Sci.* **2002**, *500*, 656–677.

(2) Ulman, A. Formation and structure of self-assembled monolayers. *Chem. Rev.* **1996**, *96* (4), 1533–1554.

(3) Nuzzo, R.; Dubois, L.; Allara, D. Fundamental studies of microscopic wetting on organic surfaces. 1. Formation and structural characterization of a self-consistent series of polyfunctional organic monolayers. *J. Am. Chem. Soc.* **1990**, *112* (2), 558–569.

(4) love, J. C.; Estroff, L. A.; Kriebel, J. K.; Nuzzo, R. G.; Whitesides, G. M. Self-assembled monolayers of thiolates on metals as a form of nanotechnology. *Chem. Rev.* **2005**, *105* (4), 1103–1170.

(5) Boujday, S.; Bantegnie, A.; Briand, E.; Marnet, P.-G.; Salmain, M.; Pradier, C.-M. In-depth investigation of protein adsorption on gold

surfaces: Correlating the structure and density to the efficiency of the sensing layer. *J. Phys. Chem. B* **2008**, *112* (21), 6708–6715.

(6) Boujday, S.; Briandet, R.; Salmain, M.; Herry, J.-M.; Marnet, P.-G.; Gautier, M.; Pradier, C.-M. Detection of pathogenic *Staphylococcus aureus* bacteria by gold based immunosensors. *Microchim. Acta* **2008**, *163* (3−4), 203–209.

(7) Boujday, S.; Gu, C.; Girardot, M.; Salmain, M.; Pradier, C.-M. Surface IR applied to rapid and direct immunosensing of environmental pollutants. *Talanta* **2009**, *78* (1), 165–170.

(8) Boujday, S.; Nasri, S.; Salmain, M.; Pradier, C.-M. Surface IR immunosensors for label-free detection of benzo[*a*]pyrene. *Biosens. Bioelectron.* **2010**, *26* (4), 1750–1754.

(9) Morel, A.-L.; Volmant, R.-M.; Méthivier, C.; Krafft, J.-M.; Boujday, S.; Pradier, C.-M. Optimized immobilization of gold nanoparticles on planar surfaces through alkyldithiols and their use to build 3D biosensors. *Colloids Surf., B* **2010**, *81* (1), 304–312.

(10) Ulman, A. *An Introduction to Ultrathin Organic Films from Langmuir-Blodgett to Self-Assembly*; Academic Press: London, 1991.

(11) Ciampi, S.; Harper, J. B.; Gooding, J. J. Wet chemical routes to the assembly of organic monolayers on silicon surfaces via the formation of Si-C bonds: Surface preparation, passivation and functionalization. *Chem. Soc. Rev* **2010**, *39* (6), 2158–2183.

(12) Gooding, J. J.; Ciampi, S. The molecular level modification of surfaces: From self-assembled monolayers to complex molecular assemblies. *Chem. Soc. Rev.* **2011**, *40*, 2704–2718.

(13) Haensch, C.; Hoeppener, S.; Schubert, U. S. Chemical modification of self-assembled silane based monolayers by surface reactions. *Chem. Soc. Rev.* **2010**, *39* (6), 2323–2334.

(14) Suzuki, N.; Ishida, H. A review on the structure and characterization techniques of silane/matrix interphases. *Macromol. Symp.* **1996**, *108* (1), 19–53.

(15) Boukherroub, R.; Morin, S.; Bensebaa, F.; Wayner, D. D. M. New synthetic routes to alkyl monolayers on the Si(111) surface. *Langmuir* **1999**, *15* (11), 3831–3835.

(16) Smith, E. A.; Chen, W. How to prevent the loss of surface functionality derived from aminosilanes. *Langmuir* **2008**, *24*, 12405–12409.

(17) Howarter, J. A.; Youngblood, J. P. Optimization of silica silanization by 3-aminopropyltriethoxysilane. *Langmuir* **2006**, *22* (26), 11142–11147.

(18) Pasternack, R. M.; Rivillon Amy, S.; Chabal, Y. J. Attachment of 3-(aminopropyl)triethoxysilane on silicon oxide surfaces: Dependence on solution temperature. *Langmuir* **2008**, *24* (22), 12963–12971.

(19) El-Ghannam, A. R.; Ducheyne, P.; Risbud, M.; Adams, C. S.; Shapiro, I. M.; Castner, D.; Golledge, S.; Composto, R. J. Model surfaces engineered with nanoscale roughness and RGD tripeptides promote osteoblast activity. *J. Biomed. Mater. Res., Part A* **2004**, *68A* (4), 615–627.

(20) Kim, J.; Seidler, P.; Wan, L. S.; Fill, C. Formation, structure, and reactivity of amino-terminated organic films on silicon substrates. *J. Colloid Interface Sci.* **2009**, *329* (1), 114–119.

(21) Weng, Y. J.; Hou, R. X.; Li, G. C.; Wang, J.; Huang, N.; Liu, H. Q. Immobilization of bovine serum albumin on $TiO_2$ film via chemisorption of $H_3PO_4$ interface and effects on platelets adhesion. *Appl. Surf. Sci.* **2008**, *254* (9), 2712–2719.

(22) Lapin, N. A.; Chabal, Y. J. Infrared characterization of biotinylated silicon oxide surfaces, surface stability, and specific attachment of streptavidin. *J. Phys. Chem. B* **2009**, *113* (25), 8776–8783.

(23) Kim, J.; Cho, J.; Seidler, P. M.; Kurland, N. E.; Yadavalli, V. K. Investigations of chemical modifications of amino-terminated organic films on silicon substrates and controlled protein immobilization. *Langmuir* **2010**, *26* (4), 2599–2608.

(24) Crampton, N.; Bonass, W. A.; Kirkham, J.; Thomson, N. Formation of aminosilane-functionalized mica for atomic force microscopy imaging of DNA. *Langmuir* **2005**, *21*, 7884–7891.

(25) Dekeyser, C. M.; Buron, C. C.; Mc Evoy, K.; Dupont-Gillain, C. C.; Marchand-Brynaert, J.; Jonas, A. M.; Rouxhet, P. G. Oligo(ethylene glycol) monolayers by silanization of silicon wafers: Real nature and stability. *J. Colloid Interface Sci.* **2008**, *324* (1−2), 118–126.

(26) Lummerstorfer, T.; Hoffmann, H. IR reflection spectra of monolayer films sandwiched between two high refractive index materials. *Langmuir* **2004**, *20* (16), 6542–6545.

(27) Lummerstorfer, T.; Hoffmann, H. Click chemistry on surfaces: 1,3-Dipolar cycloaddition reactions of azide-terminated monolayers on silica. *J. Phys. Chem. B* **2004**, *108*, 3963–3966.

(28) Lummerstorfer, T.; Kattner, J.; Hoffmann, H. Monolayers at solid-solid interfaces probed with infrared spectroscopy. *Anal. Bioanal. Chem.* **2007**, *388* (1), 55–64.

(29) Milosevic, M.; Milosevic, V.; Berets, S. L. Grazing angle attenuated total reflection spectroscopy: fields at the interface and source of the enhancement. *Appl. Spectrosc.* **2007**, *61* (5), 530–536.

(30) Ling, L.; Kuwabara, S.; Abe, T.; Shimura, F. Multiple internal-reflection infrared-spectroscopy of silicon surface-structure and oxidation process at room-temperature. *J. Appl. Phys.* **1993**, *73* (6), 3018–3022.

(31) Asay, D. B.; Kim, S. H. Evolution of the adsorbed water layer structure on silicon oxide at room temperature. *J. Phys. Chem. B* **2005**, *109* (35), 16760–16763.

(32) Kluth, G. J.; Sung, M. M.; Maboudian, R. Thermal behavior of alkylsiloxane self-assembled monolayers on the oxidized Si(100) surface. *Langmuir* **1997**, *13*, 3775–3780.

(33) Pena-Alonso, R.; Rubio, F.; Rubio, J. Study of the hydrolysis and condensation of $\gamma$-aminopropyltriethoxysilane by FT-IR spectroscopy. *J. Mater. Sci.* **2007**, *42*, 595–603.

(34) Socrates, G. *Infrared Characteristic Group Frequencies: Tables and Charts*, 2nd ed.; John Wiley & Sons: Chichester, U.K., 1994; 249 pp.

(35) Kim, J.; Seidler, P.; Fill, C.; Wan, L. S. Investigations of the effect of curing conditions on the structure and stability of amino-functionalized organic films on silicon substrates by Fourier transform infrared spectroscopy, ellipsometry, and fluorescence microscopy. *Surf. Sci.* **2008**, *602*, 3323–3330.

(36) Olsen, J. E.; Shimura, F. Infrared spectroscopy of thin sincon dioxide on silicon. *Appl. Phys. Lett.* **1988**, *53* (20), 1934–1936.

(37) Nagai, N.; Hashimoto, H. FT-IR-ATR study of depth profile of $SiO_2$ ultra-thin films. *Appl. Surf. Sci.* **2001**, *172* (3−4), 307–311.

(38) Burneau, A.; Gallas, J.-P. Vibrational spectroscopies. In *The Surface Properties of Silicas*; Legrand, A. P., Ed.; John Wiley & Sons: Chichester, U.K., 1998; Chapter 3, p 147.

(39) Iler, R. K. *The Chemistry of Silica*; Wiley-Interscience: New York, 1979.

(40) Queeney, K. T.; Herbots, N.; Shaw, J. M.; Atluri, V.; Chabal, Y. J. Infrared spectroscopic analysis of an ordered $Si/SiO_2$ interface. *Appl. Phys. Lett.* **2004**, *84* (4), 493–495.

(41) Queeney, K. T.; Weldon, M. K.; Chang, J. P.; Chabal, Y. J.; Gurevich, A. B.; Sapjeta, J.; Opila, R. L. Infrared spectroscopic analysis of the $Si/SiO_2$ interface structure of thermally oxidized silicon. *J. Appl. Phys.* **2000**, *87* (3), 1322–1330.

(42) Tian, R.; Seitz, O.; Li, M.; Hu, W.; Chabal, Y. J.; Gao, J. Infrared characterization of interfacial Si−O bond formation on silanized flat $SiO_2/Si$ surfaces. *Langmuir* **2010**, *26* (7), 4563–4566.

(43) Vandenberg, E. T.; Bertilsson, L.; Liedberg, B.; Uvdal, K.; Erlandsson, R.; Elwing, H.; Lundström, I. Structure of 3-aminopropyl triethoxy silane on silicon oxide. *J. Colloid Interface Sci.* **1991**, *147*, 103–118.

(44) Kurth, D. G.; Bein, T. Thin films of (3-aminopropyl)triethoxysilane on aluminum oxide and gold substrates. *Langmuir* **1995**, *11* (8), 3061–3067.

(45) Remes, Z.; Kromka, A.; Vanecek, M.; Grinevich, A.; Hartmannova, H.; Kmoch, S. The RF plasma surface chemical modification of nanodiamond films grown on glass and silicon at low temperature. *Diamond Relat. Mater.* **2007**, *16* (4−7), 671–674.

(46) Rochat, N.; Chabli, A.; Bertin, F.; Olivier, M.; Vergnaud, C.; Mur, P. Attenuated total reflection spectroscopy for infrared analysis of thin layers on a semiconductor substrate. *J. Appl. Phys.* **2002**, *91* (8), 5029–5034.

(47) Culler, S. R.; Naviroj, S.; Ishida, H.; Koenig, J. L. Analytical and Spectroscopic Investigation of the Interaction of Carbon Dioxide with

Amine Functional Silane Coupling Agents; Case Western Reserve University: Cleveland, OH, 1982; 36 pp.

(48) Hook, F.; Voros, J.; Rodahl, M.; Kurrat, R.; Boni, P.; Ramsden, J. J.; Textor, M.; Spencer, N. D.; Tengvall, P.; Gold, J.; Kasemo, B. A comparative study of protein adsorption on titanium oxide surfaces using in situ ellipsometry, optical waveguide lightmode spectroscopy, and quartz crystal microbalance/dissipation. *Colloids Surf., B* **2002**, *24* (2), 155–170.

(49) Hook, F.; Kasemo, B.; Nylander, T.; Fant, C.; Sott, K.; Elwing, H. Variations in coupled water, viscoelastic properties, and film thickness of a Mefp-1 protein film during adsorption and cross-linking: a quartz crystal microbalance with dissipation monitoring, ellipsometry, and surface plasmon resonance study. *Anal. Chem.* **2001**, *73* (24), 5796–804.

(50) Boujday, S.; Lambert, J.-F.; Che, M. Evidence for interfacial molecular recognition in transition metal complexes adsorption on amorphous silica surfaces. *J. Phys. Chem. B* **2003**, *107* (3), 651–654.

(51) Boujday, S.; Lambert, J.-F.; Che, M. Amorphous silica as a versatile supermolecular ligand for NiII amine complexes: Toward interfacial molecular recognition. *ChemPhysChem* **2004**, *5* (7), 1003–1013.

(52) White, L. D.; Tripp, C. P. Reaction of (3-aminopropyl)dimethylethoxysilane with amine catalysts on silica surfaces. *J. Colloid Interface Sci.* **2000**, *232* (2), 400–407.